Journal of Materials Science and Engineering B 6 (7-8) (2016) 201-210
doi: 10.17265/2161-6221/2016.7-8.006

Growth Process Improvement for Casting High-Performance Multi-Crystalline Silicon Ingots for Solar Cells

Wenliang Chen[1], Bing Zhou[1], Junjing Ding[1], Yunyang Yu[1], Hui Dong[2], Genxiang Zhong[3] and Xinming Huang[1, 3*]

1. School of Materials Science and Engineering, Nanjing Tech University, Nanjing, Jiangsu 21009, China

2. Donghai JA Solar Technology Co., Ltd., Lianyungang, Jiangsu 222300, China

3. JA Solar Holdings Co., Ltd., Feng Tai District, Beijing 100160, China

Abstract: An improved growth process was proposed to produce the high-quality multi-crystalline silicon ingots for solar cells. A transient numerical model was used to investigate the effects of the growth process design parameters on the crystal-melt (c-m) interface, the melt convection and the thermal stress distribution during the growth process. The simulation results showed that compared with the original design, the almost flat c-m interface, the favorable melt convection and the much lower thermal stress were obtained with the improved design. Ingot casting experiments were performed for the two designs. The average yield rate of silicon ingots was 3.69% higher in absolute value with the improved design, and the interstitial oxygen content of silicon wafers was lower. The average conversion efficiency of p-type solar cells was 0.18% higher in absolute value with the improved design (18.59%) than that with the original design (18.41%).

Key words: Computer simulation, directional solidification, heat transfer, industrial crystallization, solar cells.

1. Introduction

The photovoltaic industry is witnessing a strong development momentum, and the Multi-crystalline silicon (mc-Si) occupies the largest market share. Directional solidification (DS) has emerged as a key production technology for the growth of mc-Si ingots over past decade because of its cost-effectiveness. Many new DS techniques have been developed for the seed-assisted growth for the High-performance (HP) mc-Si ingots [1, 2], and the seeds consist of homo-seeds [3, 4] or hetero-seeds [5,6] in the HP mc-Si industrial production. The quality of silicon ingots is significantly affected by the thermal history of the growth process, such as the evolution of the crystal-melt (c-m) interface shape [7, 8], melt convection pattern [9, 10] and thermal stress distribution [11, 12]. To achieve the higher performance of HP mc-Si solar cells and market share, it is very necessary to optimize the DS process, including the furnace configurations and the process operating parameters in the industrial furnace.

In this paper, an improved growth process design was proposed to produce the HP mc-Si silicon ingots in an industrial DS furnace. A transient numerical model was applied to compare the c-m interface shape, melt convection pattern and thermal stress distribution between the improved design and the original design. Ingot casting experiments were also performed for the two designs. The infrared image of silicon bricks, the yield rate of silicon ingots, the interstitial oxygen content of silicon wafers and the conversion efficiency of p-type solar cells were compared in this work.

*[*]**Corresponding author:** Xinming Huang, Ph.D., professor of photovoltaic materials, research fields: silicon crystal growth and solar cell.

2. Materials

2.1 Model Description

The JJL500 DS system used in the experiments is shown in Fig. 1. It consists of top and side graphite heaters, a quartz crucible, a graphite susceptor, a heat exchange block, a gas shield, insulations, thermocouples, and a movable insulation partition block. The functions of the system components and the operating conditions have been described in our previous study [13]. Specially processed quartz granules (hetero-seeds) were first paved across the entire bottom of crucible with a volume of 890 × 890 × 480 mm^3, and then a Si_3N_4 layer was coated on the inner wall of the crucible. About 520-kg Si feedstock was loaded into the prepared crucible to produce a silicon ingot with a height of 310 mm.

The CGSim transient global model was used for the simulations presented in this paper, and it has been verified in our previous studies [13, 14]. In the numerical model, the furnace was assumed to be a 2-D axisymmetric based on the real DS system, and the model took into account the thermal conduction, thermal radiation, melt convection and gas flow. The melt was regarded as a Newtonian fluid, and the inert argon gas was treated as an ideal gas and incompressible, and all of the radiative surfaces were assumed to be diffuse gray. Other descriptions of the model have been given in our previous publications, including the numerical mesh settings of each furnace part [13], the physical parameter settings of each material [13] and the algebraic turbulence model for melt convection [15]. The temperature at the crystallization interface was set to 1,685 K, a steady global simulation was first performed, and then an unsteady global simulation was performed to simulate crystal growth. The dynamic front tracking method was adopted to track the position of the interface. The thermo-elastic stress model was applied to analyze the thermal stress distribution in the silicon crystal during the solidification process [15-17]. The crystal was assumed to be isotropic and the Von Mises stress was used to reflect the thermal stress.

2.2 Process Improvement Design

In our previous studies, the insulation partition block [14] and the variable power ratio between the top and side heaters [15] had significant effects on the thermal field in the furnace. Based on their advantages, we proposed an improved growth process to better

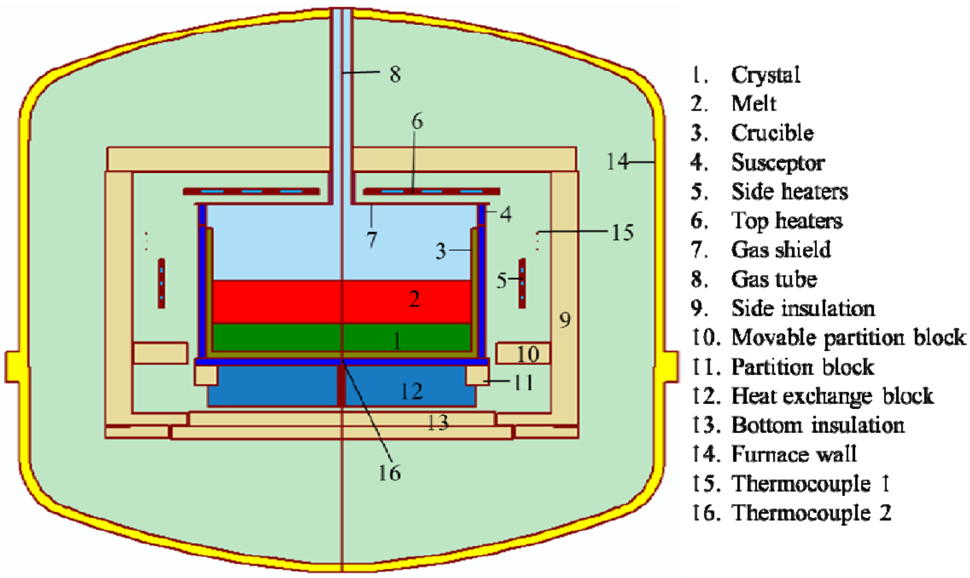

Fig. 1 Configuration of the DS furnace.

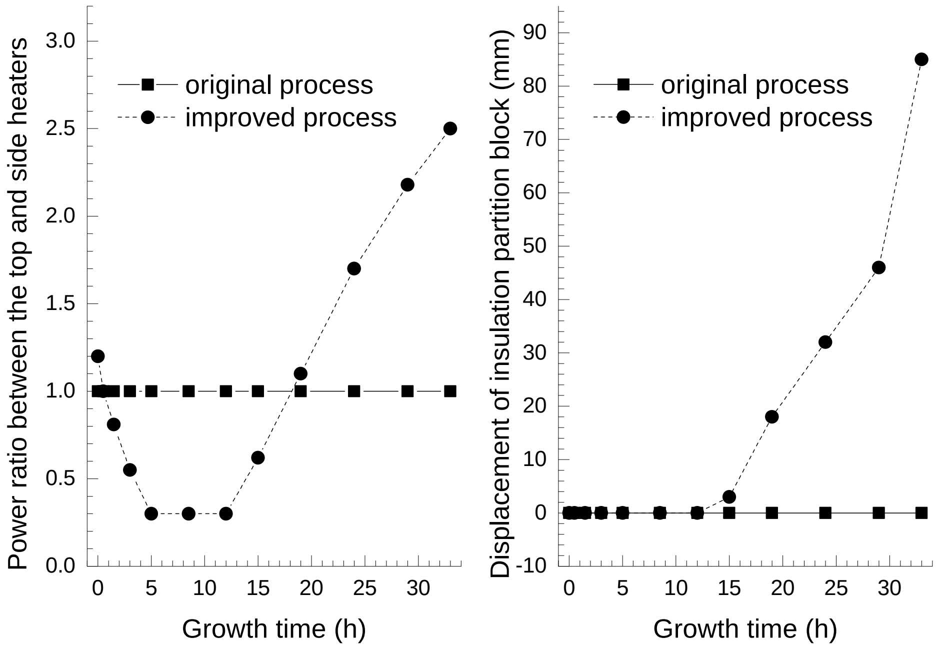

Fig. 2 Parameters of the growth process for the two designs.

control the thermal field throughout the solidification process. Fig. 2 shows the specific prescribed growth process parameters for both the power ratio and the position of the insulation partition block. In the original design, the power ratio was fixed at 1 : 1, and the partition block was fixed near the susceptor (index 10 in Fig. 1). In the improved design, the power ratio first decreased from 1.2 to 0.3 at 5th hour, and then the power ratio of 0.3 lasted for 7 hours, next, it increased up to 2.5 at 33th hour; meanwhile, the partition block was motionless from 0 to 12th hour and then moved up to 85 mm at 33th hour (the upward direction was defined as the positive direction). Apart from the power ratios and the position of partition block, all other conditions were kept identical during the growth process in the two cases.

3. Results and Discussion

3.1 Comparison of C-M Interface Shape

A flat or slightly convex c-m interface is beneficial for pushing impurities outwards and preventing nucleation at the side wall of the crucible. Fig. 3 shows the horizontal deflections of the c-m interface with the growth height for the two processes. The deflection is defined as the interface height difference between the central and the outermost edge regions. A positive deflection represents a convex interface shape (i.e., the interface is convex toward the melt), conversely, a concave interface shape. For the original design, the c-m interface transformed from convex to concave at the early stage of solidification, such a transformation was not beneficial for the growth of high-quality crystal [7]. The deflections were very large at the later stage of growth, and the higher thermal stress probably occurred in the edge regions due to the large radial temperature gradient. The c-m interface always was almost flat during the entire solidification process in the improved design. These observations can be explained as follows. In the improved design, the power ratio of slightly greater than 1 at the initial stage of solidification was beneficial to decrease the deflection of a convex interface [15]; and then the power ratio was less than 1, the edge regions temperature gradually increased, which avoided the interface transforming from convex to concave and maintained an almost flat interface; next, the power ratio was greater than 1 and the partition block moved

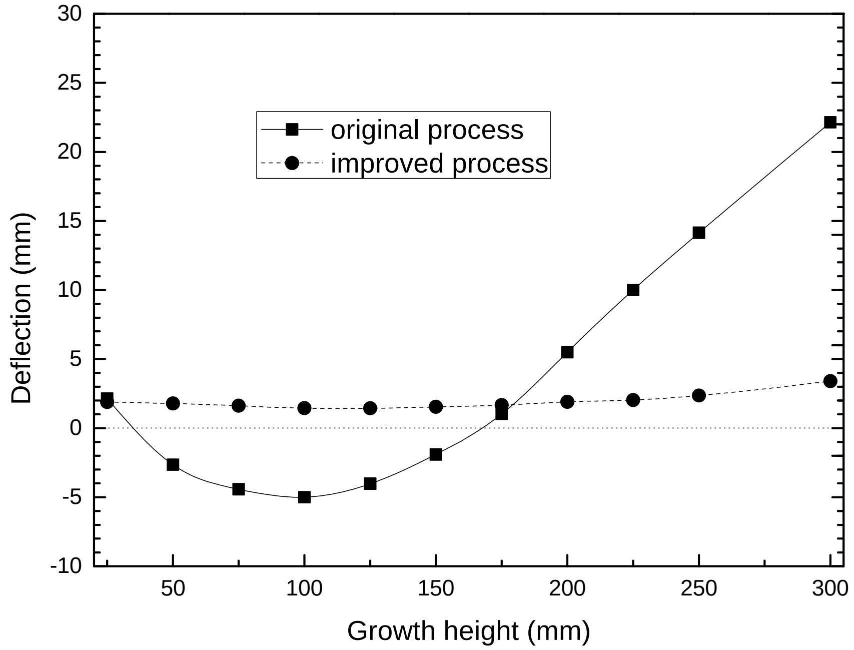

Fig. 3 Deflection of the c-m interface with the growth height for the two designs.

upwards, the edge regions temperature gradually decreased, and then the growth rate of edge regions appropriately increased, which kept the interface almost flat and then just slightly convex.

3.2 Comparison of Melt Convection

A low oxygen concentration is beneficial to suppress the light induced degradation of solar cells. Fig. 4 shows the temperature and the melt convection distributions of the melt for the two designs. The left and right side of these figures reveal the temperature distribution and the melt convection in the melt, respectively. For a solidification fraction of 30%, there were two main convection cells in the two designs; the fluid flows of the convection cell at the lower position of the melt moved downward along the crucible wall, and the fluid flows at the upper position moved upward along the crucible wall, as shown in Fig. 4a. Compared with the original design, the convection cell at the lower position was weaker-strength and smaller-dimension in improved design because of the smaller radial temperature gradient, and it was much stronger-strength and larger-dimension at the upper position because of the larger radial temperature gradient, which was beneficial to reduce oxygen impurities concentration in the central regions [9]. For a solidification fraction of 60%, there still were two main convection cells in the original design, although the number of convection cells in improved design became four due to the smaller axial temperature gradient in the central regions. In the improved design, the fluid flows at the interface front moved from the center to edge, as shown in Fig. 4b (indicated by the red dashed rectangle), and the convection cell at the bottom corner regions of the melt was much weaker-strength, apparently the oxygen impurities in the central regions can be pushed outwards. These results indicated that a favorable melt convection distribution for the crystal growth could be obtained with the improved design.

3.3 Comparison of Thermal Stress

Many studies have shown that high thermal stress likely occurred in the central and edge regions of the silicon crystal [12, 14, 15], which indicated a W-type stress distribution in the crystal. A W-type stress

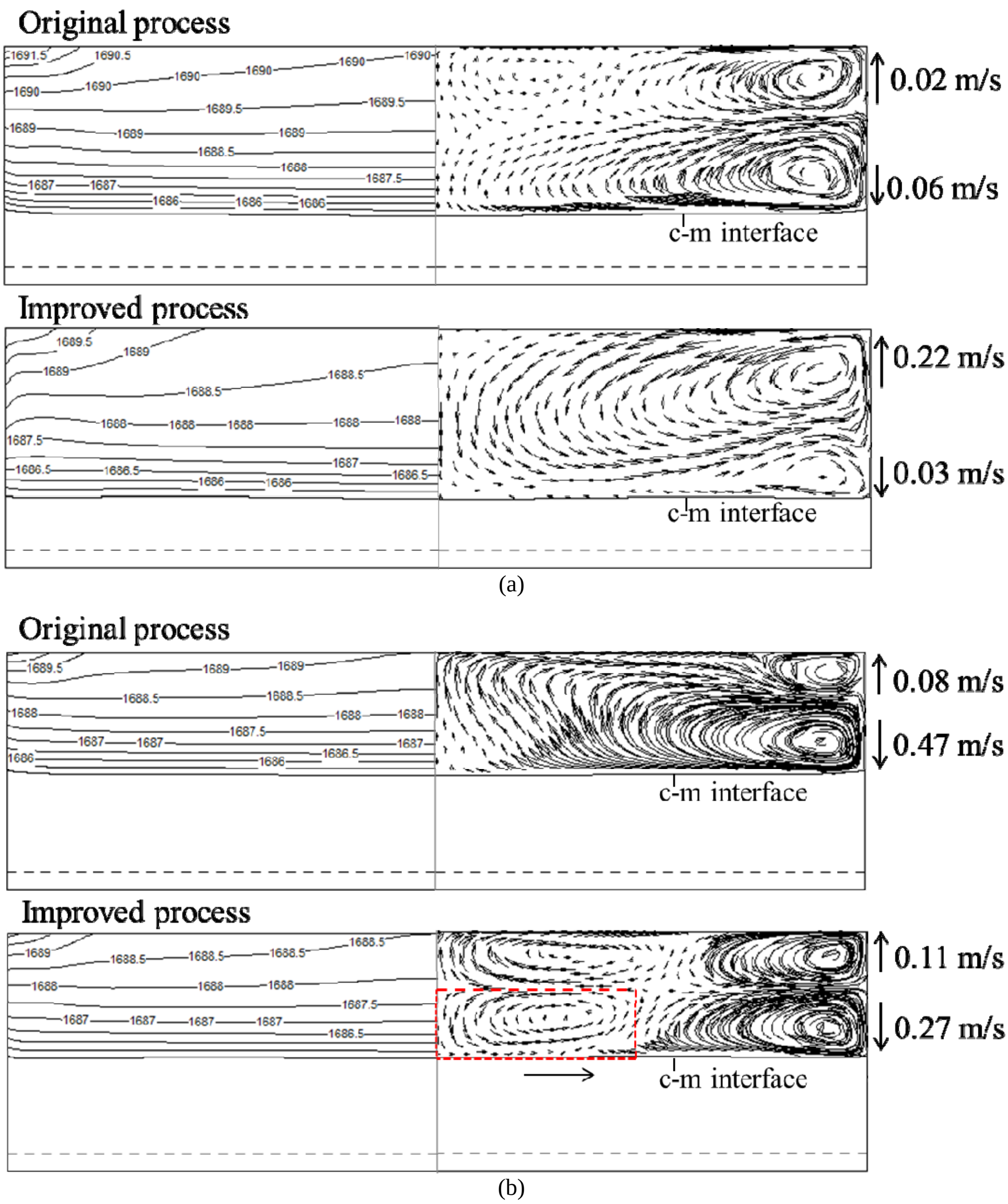

Fig. 4 Temperature (left, interval of 0.5 K) and melt convection (right) distributions for the two designs with solidified fractions of (a) 30% and (b) 60%.

distribution also occurred in the two designs. The evolution of the highest Von Mises stress with the growth time in both the central and the edge regions was shown in Fig. 5a. For the two designs, the highest-stress occurred in the central regions in the first half of growth time, and the highest-stress occurred in the edge regions at the latter half. The highest-stress in both the central and the edge regions was lower at the later stage of growth for the improved design compared with the original design, especially in the edge regions. Fig. 5b shows the transient temperature and thermal stress distribution in the crystal with the solidified time of 33 h, the left and right side of these figures reveal the temperature and thermal stress distribution in the crystal, respectively. Compared with the original design, the radial temperature gradient was much smaller in the improved design, and the axial temperature gradient was

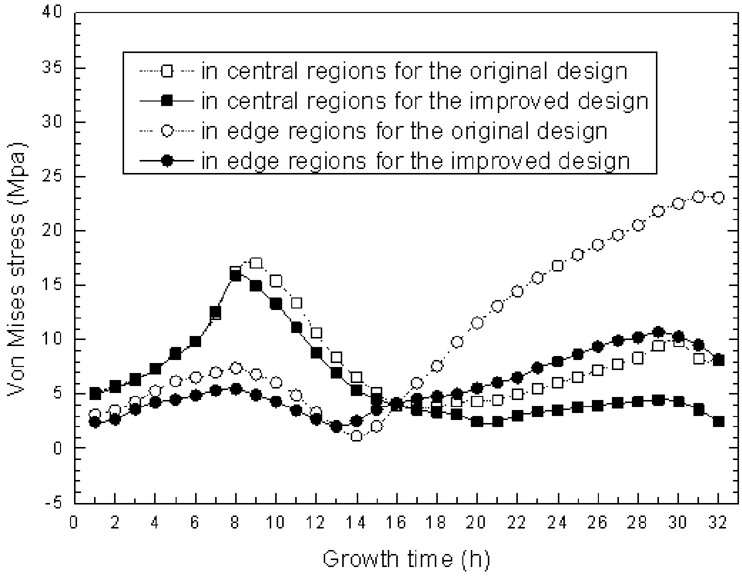

(a)

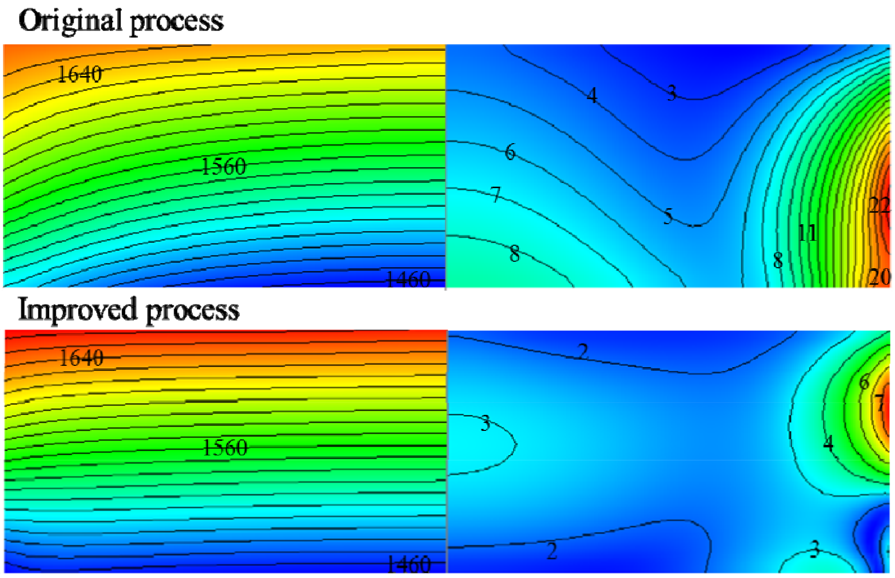

(b)

Fig. 5 (a) Evolution of the highest Von Mises stress with the growth time in both the central and edge regions of the crystal, (b) Temperature (left, interval of 10 K) and thermal stress (right, Von Mises stress, interval of 1 MPa) distributions with the solidified time of 33 h.

larger. There was a high stress area in the edge regions at the height of about 90-101 mm away from the crucible bottom for the original design, and at the height of about 200-05 mm for the improved design. However, the highest-stress in the edge regions with the improved design (7.4 MPa) was about 15.1 MPa lower than that with the original design (22.5 MPa). The simulation results revealed that the thermal stress of the crystal can be significantly reduced in the improved design due to the much smaller radial temperature gradient, while the axial temperature gradient was larger. This means that the decrease in the radial temperature gradient played a leading role in the decrease of the thermal stress. Lowering the thermal stress is beneficial to improve the quality of crystal.

3.4 Experimental Results

The original and improved growth process designs were employed in casting experiments. Each ingot was cut into 25 bricks, as shown in Fig. 6a. Figs. 6b and 6c show the infrared images of the front view of brick B11 for the original and improved designs, respectively. The infrared images of the front view of brick C13 for the original and improved designs are shown in Figs. 6d and 6e, respectively. In the original design, the grains first grew inward along the side wall of the crucible and then grew outward, as shown in Fig. 6b (indicated by the black arrows); thus, the c-m interface was inferred to be first concave and then convex with crystal growth. In the improved design, the grains grew straight up, as shown in Fig. 6c (indicated by the black arrow), and the c-m interface was inferred to be almost flat during the entire growth process. These inferred results agreed with the simulation results shown in Fig. 3.

Some shadow regions sometimes appeared in a silicon ingot, which definitely decreases the yield rate of silicon ingots [12, 18]. In the original design, the shadow regions almost always appeared in the silicon bricks B11 and C13, as shown in Figs. 6b and 6d (indicated by the black rectangles); while it almost disappeared in the improved process, as shown

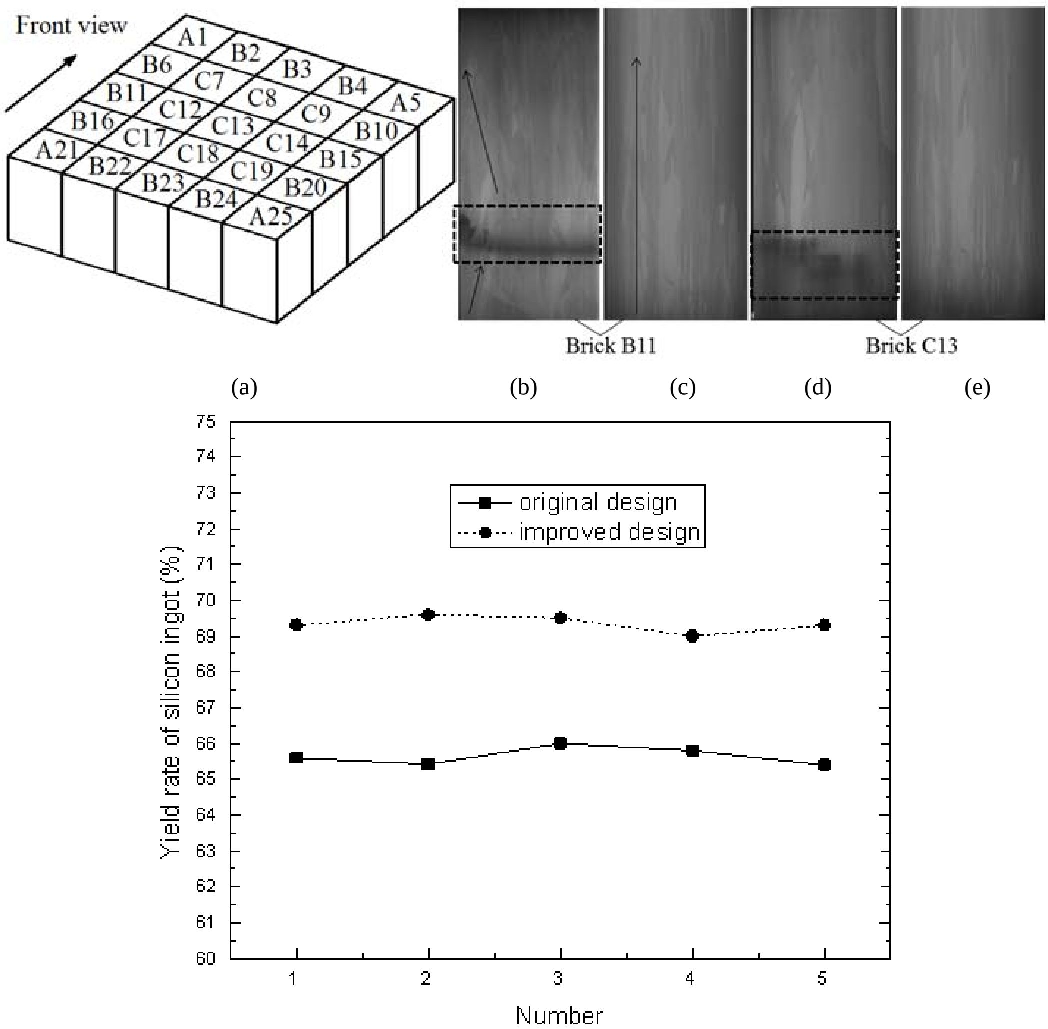

(f)

Fig. 6 (a) Numbering of bricks from an ingot, (b)-(e) infrared images of the silicon bricks for the two designs, (b) and (d) the original design, (c) and (e) the improved design, (f) yield rates of silicon ingots for the two designs.

in Figs. 6c and 6e. This were probably benefited from the much lower thermal stress in the edge regions and the lower impurities concentration in the central regions for the improved design compared with the original design. To compare the yield rate of silicon ingots for the two designs, five experimental results from the two designs were summarized, as shown in Fig. 6f. The average yield rate of silicon ingots was 3.69% higher in absolute value with the improved design (69.32%) than that with the original design (65.63%). This 3.69% increase in yield rate of silicon ingot was a great improvement of the number of silicon wafers, corresponding to an extra about 950 silicon wafers with a thickness of 0.18 mm in a silicon ingot. The improved growth process was beneficial to reduce the shadow regions and improve the yield rate of silicon ingots.

After removing the red zone, the interstitial oxygen contents of silicon wafers at the same height of the brick C13 were compared for the two designs, as shown in Fig. 7. The interstitial oxygen content in the improved design was lower than that in the original design, the results benefited from the almost flat c-m interface shape and the favorable melt convection distribution.

The 7200 silicon wafers with a width of 156 mm chosen from regions A, B and C at the ratio of 4 : 12: 9 for each ingot (the same ratio of all the bricks in the whole ingot) were used respectively to fabricate p-type solar cells using the same standard manufacture technique. Fig. 8 shows the conversion efficiency of solar cells for the two designs. The conversion efficiency mainly concentrated in the range of 18.3-18.5 for the original design, and it mainly concentrated in the range of 18.5-18.7 for the improved design. The average conversion efficiency of HP mc-Si solar cells was 0.18% higher in absolute value with the improved design (18.59%) than that with the original design (18.41%). The 0.18% increase in conversion efficiency of solar cells was an effective improvement of conversion efficiency in mass production, corresponding to an extra 3 W of output power in a standard module with 72 solar cells.

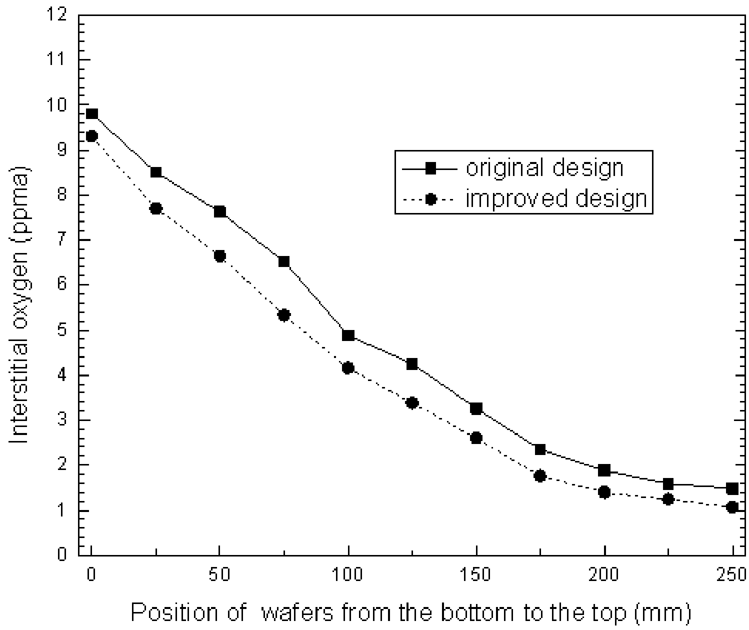

Fig. 7 Interstitial oxygen distribution along the growth direction of the brick C13 for the two designs.

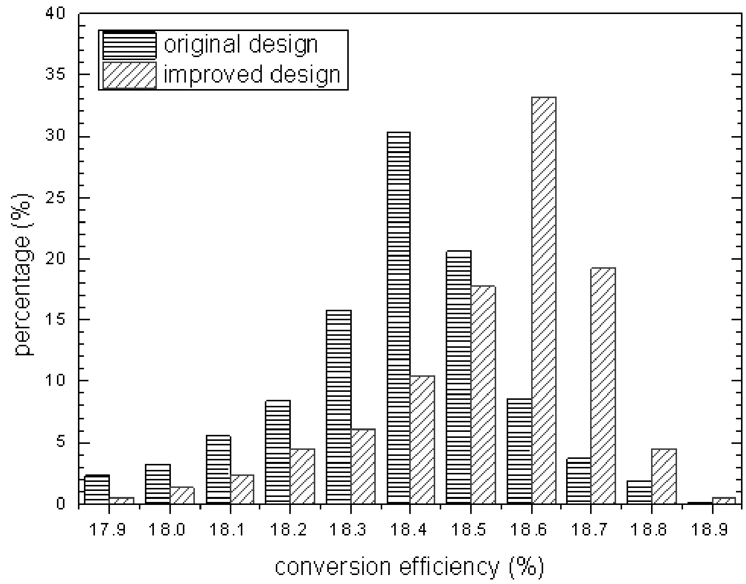

Fig. 8 Conversion efficiency of solar cells for the two designs.

4. Conclusions

An improved growth process design was proposed to produce high-quality mc-Si ingots. The simulation results showed that the almost flat c-m interface, the favorable melt convection and the much lower thermal stress were obtained with the improved design. Experimental results showed that the improved process design was the optimal growth process, because a vertical columnar structure and a lower interstitial were achieved with the improved design. In the improved process, the average yield of silicon ingots was 3.69% higher in absolute value, and the average conversion efficiency of solar cells was 0.18% higher in absolute value with the improved design than that with the original design. These increases were great improvements in a silicon ingot. In addition, this study was an important reference for growing high-quality mc-Si ingots in an upgraded generation-six (G6) DS furnace from a G5 one.

Acknowledgments

This work was partly supported by the Program for Changjiang Scholars and Innovative Research Team in University (PCSIRT) under grant no. IRT1146; a project funded by the Priority Academic Program Development of Jiangsu Higher Education Institutions (PAPD); a project funded by the Natural Science Foundation of the Jiangsu Higher Education Institutions under grant no. 13KJB430016; and a project funded by the Natural Science Foundation of the Jiangsu province under grant no. BK20141460.

References

[1] Lan, C. W., Hsu, C. and Nakajima, K. 2015. "Multicrystalline Silicon Crystal Growth Photovoltaic Applications." *Handbook of Crystal Growth (Second Edition): Bulk Crystal Growth* 10: 373-411.

[2] Lan, C. W., Yang, C. F., Lan, A., Yang, M., Yu, A., Hsu, H. P., Hsu, B. and Hsu, C. 2016. "Engineering Silicon Crystals for Photovoltaics." *CrystEngComm* 18 (January): 1474-85.

[3] Lan, C. W., Yu, W. H., Yang, Y. M., Chou, H. S., Chen,Y. L., Hsu, C. L. and Hsu, W. C. 2014. "Crystalline Silicon Ingot and Silicon Wafer Therefrom." ROC Pat. TW1452185B.

[4] Zhu, D. D., Ming, L., Huang, M. L., Zhang, Z. Y. and Huang, X. M. 2014. "Seed-Assisted Growth of High-Quality Multi-Crystalline Silicon in Directional Solidification." *Journal of Crystal Growth* 386 (January): 52-6.

[5] Zhang, H. L., You, D., Huang, C. L., Wu, Y. H., Xu, Y. and Wu, P. 2016. "Growth of Multicrystalline Silicon Ingot with Both Enhanced Quality and Yield Through Quartz Seeded Method." *Journal of Crystal Growth* 435 (February): 91-7.

[6] Ding, J. J., Yu, Y. Y., Chen, W. L., Zhou, X. C., Wu, Z. Y., Zhong, G. X. and Huang, X. M. 2016. "Effect of the Fused Quartz Particle Density on Nucleation and Grain Control of High-Performance Multicrystalline Silicon Ingots." *Journal of Crystal Growth* 454 (November): 186-91.

[7] Franke, D., Rettelbach, T., Häßler, C., Koch, W. and Müller, A. 2002. "Silicon Ingot Casting: Process Development by Numerical Simulations." *Solar Energy Materials and Solar Cells* 72 (April): 83-92.

[8] Wu, B., Stoddard, N., Ma, R. H. and Clark, R. 2008. "Bulk Multicrystalline Silicon Growth for Photovoltaic (PV) Application." *Journal of Crystal Growth* 310 (April): 2178-84.

[9] Teng, Y. Y., Chen, J. C., Lu, C. W. and Chen, C. Y. 2010. "The Carbon Distribution in Multicrystalline Silicon Ingots Grown Using the Directional Solidification Process." *Journal of Crystal Growth* 312 (April): 1282-90.

[10] Bellmann, M. P., Meese, E. A. and Arnberg, L. 2010. "Impurity Segregation in Directional Solidified Multi-Crystalline Silicon." *Journal of Crystal Growth* 312 (October): 3091-5.

[11] Nakano, S., Chen, X. J., Gao, B. and Kakimoto, K. 2011. "Numerical Analysis of Cooling Rate Dependence on Dislocation Density in Multicrystalline Silicon for Solar Cells." *Journal of Crystal Growth* 318 (March) 280-2.

[12] Qi, X. F., Yu, Q. H., Zhao, W. H., Liang, X. Q., Zhang, J. and Liu, L. J. 2014. "Improved Seeded Directional Solidification Process for Producing High-Efficiency Multi-Crystalline Silicon Ingots for Solar Cells." *Solar Energy Materials and Solar Cells* 130 (November): 118-23.

[13] Ding, C. L., Huang, M. L., Zhong, G. X., Ming, L. and Huang, X. M. 2014. "A Design of Crucible Susceptor for the Seeds Preservation During a Seeded Directional Solidification Process." *Journal of Crystal Growth* 387 (February): 73-80.

[14] Wu, Z. Y., Zhong, G. X,. Zhang, Z. Y., Zhou, X. C., Wang, Z. X. and Huang, X. M. 2015. "Optimization of the High-Performance Multi-crystalline Silicon Solidification Process by Insulation Partition Design Using Transient Global Simulations." *Journal of Crystal Growth* 426 (September): 110-6.

[15] Chen, W. L., Wu, Z. Y., Zhong, G. X., Ding, J. J., Yu, Y. Y., Zhou, X. C. and Huang, X. M. 2016. "Optimization of Heat Transfer by Adjusting Power Ratios between Top and Side Heaters for Casting High-Performance Multi-Crystalline Silicon Ingots." *Journal of Crystal Growth* 451 (October): 155-60.

[16] Black, A., Medina, J., Piñeiro, A. and Dieguez, E. 2012. "Optimizing Seeded Casting of Mono-like Silicon Crystals through Numerical Simulation." *Journal of Crystal Growth* 353 (August): 12-6.

[17] Chen, X. J., Nakano, S., Liu, L. J. and Kakimoto, K. 2008. "Study on Thermal Stress in a Silicon Ingot during a Unidirectional Solidification Process." *Journal of Crystal Growth* 310 (September):4330-5.

[18] Ma, W. C., Zhong, G. X., Sun, L., Yu, Q. H., Huang, X. M. and Liu, L. J. 2012. "Influence of an Insulation Partition on a Seeded Directional Solidification Process for Quasi-Single Crystalline Silicon Ingot for High-Efficiency." *Solar Energy Materials and Solar Cells* 100 (May): 231-8.